Miyagi, Y., and Osaka, H. (2006). Aberrant trafficking of a proteolipid protein in a mild Pelizaeus-Merzbacher disease. Neuroscience *141*, 1861-1869.

7. Sato, A., Arimura, Y., Manago, Y., Nishikawa, K., Aoki, K., Wada, E., Suzuki, Y., Osaka, H., Setsuie, R., Sakurai, M., *et al.* (2006). Parkin potentiates ATP-induced currents due to activation of P2X receptors in PC12 cells. J Cell Physiol.
8. Setsuie, R., Wang, Y. L., Mochizuki, H., Osaka, H., Hayakawa, H., Ichihara, N., Li, H., Furuta, A., Sano, Y., Sun, Y. J., *et al.* (2006). Dopaminergic neuronal loss in transgenic mice expressing the Parkinson's disease-associated UCH-L1 I93M mutant. Neurochem Int.
9. Sun, Y. J., Nishikawa, K., Yuda, H., Wang, Y. L., Osaka, H., Fukazawa, N., Naito, A., Kudo, Y., Wada, K., and Aoki, S. (2006). Solo/Trio8, a membrane-a ssociated short isoform of Trio, modulates endosome dynamics and neurite elongation. Mol Cell Biol *26*, 6923-6935.
10. Wang, Y. L., Liu, W., Sun, Y. J., Kwon, J., Setsuie, R., Osaka, H., Noda, M., Aoki, S., Yoshikawa, Y., and Wada, K. (2006). Overexpression of ubiquitin carboxyl-terminal hydrolase L1 arrests spermatogenesis in transgenic mice. Mol Reprod Dev *73*, 40-49.
11. Takahashi, Y, Matsuda, K, Kubota Y, Shimomura J, Yamasaki, E, Kudo, T, Fukushima K, Osaka H, Akasaka N, Imamaura, A, Yamada, S, Kondo, N, Fujiwara, T(2006) Vaccination and infection as causative factors in Japanese patients with Rasmussen syndrome: Molecular mimicry and HLA class I *Clinical & Developmental Immunology*, 13: 381–387
12. **Inoue K,** Ohyama T, Sakuragi Y, Yamamoto R, Inoue NA, Yu L-H, Goto YI, Wegner M, Lupski JR. Translation of SOX10 3' untranslated region causes a complex severe neurocristopathy by generation of a deleterious functional domain. *Hum Mol Genet.* 2007;16:3037-46. (corresponding author)
13. Kim, B. Y. and Akazawa, C.

Endosomal trafficking of EGFR regulated by hVps18 via interaction of MVB sorting machinery. **Biochem. Biophys. Res. Comm.** *in press.*

14. Osaka H, Ogiwara I, Mazaki E, Okamura N,Yamashita S, Iai M, et al. Patients with a sodium channel alpha 1 gene mutation show wide phenotypic variation. Epilepsy Res 2007; 75: 46-51.
15. Setsuie R, Wang YL, Mochizuki H, Osaka H, Hayakawa H, Ichihara N, et al. Dopaminergic neuronal loss in transgenic mice expressing the Parkinson's disease-associated UCH-L1 I93M mutant. Neurochem Int 2007; 50: 119-29.
16. Tohyama J, Akasaka N, Osaka H, Maegaki Y, Kato M, Saito N, et al. Early onset West syndrome with cerebral hypomyelination and reduced cerebral white matter. Brain Dev 2008;30(5):349-55
17. Hirano R, Interthal H, Huang C, Nakamura T, **Deguchi K**, Choi K, Bhattacharjee MB, Arimura K, Umehara F, Izumo S, Northrop JL, Salih MAM, **Inoue K**, Armstrong DL, Champoux JJ, Takashima H, Boerkoel CF. Spinocerebellar ataxia with axonal neuropathy: consequence of a Tdp1 recessive neomorphic mutation? *EMBO J.* 2007;26:4732-43.
18. Takano K, Nakagawa E, **Inoue K**, Kamada F, Kure S, Goto YI A loss-of-function mutation in the *FTSJ1* gene causes nonsyndromic X-linked mental retardation in a Japanese family. Am J Med Genet B Neuropsychiatr Genet. 2008 Am J Med Genet B Neuropsychiatr Genet.; 147B(4): 479-84
19. **Deguchi K**, Clewing JM, Elizondo LI, Hirano R, Huang C, Choi K, Sloan EA, Lücke T, Marwedel KM, Powell RD, SantaCruz K, Willaime-Morawek S, **Inoue K**, Lou S, Northrop JL, Kanemura Y, van der Kooy D, Okano H, Armstrong DL, Boerkoel CF. Neurological phenotype of Schimke immuno-osseous dysplasia and neurodevelopmental expression of SMARCAL1. *J Neuropath Exp Neurol* 2008;67:565-77
20. Hashimoto M, Ishii K, Nakamura Y, Watabe K, Kohsaka

S, Akazawa C. Neuroprotective effect of sonic hedgehog up-regulated in Schwann cells following sciatic nerve injury. (2008) **J Neurochem.** 107(4):918-27.

21. Liang C, Lee JS, Inn KS, Gack MU, Li Q, Roberts EA, Vergne I, Deretic V, Feng P, Akazawa C, Jung JU. Beclin1-binding UVRAG targets the class C Vps complex to coordinate autophagosome maturation and endocytic trafficking. (2008) **Nat Cell Biol.**10(7):776-87.
22. 志村健作、石井邦弥、松尾望、赤澤智宏 BAC トランスジェニックマウス作成法を用いた Neural Crestopathy（神経堤関連疾患）解析の新規モデルマウス作成 順天堂医学 in press.
23. Goto, A., Wang, Y. L., Kabuta, T., Setsuie, R., Osaka, H., Sawa, A., Ishiura, S., and Wada, K. (2008). Proteomic and histochemical analysis of proteins involved in the dying-back-type of axonal degeneration in the gracile axonal dystrophy (gad) mouse. Neurochem Int.
24. Saitsu, H., Kato, M., Mizuguchi, T., Hamada, K., Osaka, H., Tohyama, J., Uruno, K., Kumada, S., Nishiyama, K., Nishimura, A., *et al.* (2008). De novo mutations in the gene encoding STXBP1 (MUNC18-1) cause early infantile epileptic encephalopathy. Nat Genet *40*, 782-788.
25. Tanaka, M., Hamano, S., Sakata, H., Adachi, N., Kaga, K., Osaka, H., and Kurosawa, K. (2008). Discrepancy between auditory brainstem responses, auditory steady-state responses, and auditory behavior in two patients with Pelizaeus-Merzbacher disease. Auris Nasus Larynx *35*, 404-407.
26. Elizondo LI, Cho KS, Zhang W, Yan J, Huang C, Huang Y, Choi K, Sloan EA, Deguchi K, Lou S, Baradaran-Heravi A, Takashima H, Lücke T, Quiocho FA, Boerkoel CF. Schimke immuno-osseous dysplasia: SMARCAL1 loss-of-function and phenotypic correlation. J Med Genet. 2009;46(1):49-59.

【総説】

1. 赤澤智宏、高坂新一. 末梢神経の再生におけるソニックヘッジホッグの

役割. **BRAIN and NERVE**、第 59 巻、1341-1346、2007.

2. 小坂仁、黒澤健司、井合瑞江、山下純正. Pelizaeus-Merzbacher 病の遺伝子診断　69 巻、神経内科　印刷中

【著書】

1. Inoue K. Pelizaeus-Merzbacher disease and spastic paraplegia type 2: mechanistic similarities with and differences from Charcot-Marie-Tooth disease type 1A/heredirary neuropathy with liability to pressure palsies. In Stankiewicz P, Lupski JR, eds. Genomic Disorder: The Genomic Basis of Disease. Humana Press. Totowa, NJ. 2006;263-272
2. 井上　健　遺伝子治療の最前線　編集：有馬正高、加我牧子、稲垣真澄　小児神経学　2008　診断と治療社　p510-511
3. 小坂　仁 Pelizaeus-Merzbacher 病;小児中枢神経疾患の画像診断 2008 東京医学社 484-485
4. Osaka, H., Mazaki, E., Okamura, N., Iai, M., Yamada, M., Yamakawa, K., Yamashita, S. Distinct clinical course of epilepsy with an scn2a mutation-comparison with scn1a mutations. Biology of Seizure Susceptibility in Developing Brain. Progress in Epileptic Disorders Series, Vol. 6 Takao Takahashi, Yukio Fukuyama, John Libbey Eurotext, Montrouge (Paris), France 87-100

（2）　学会発表

1. K. Inoue, M. Khajavi, T. Ohyama, C. Akazawa, J.R. Lupski. PCWH–molecular mechanisms for SOX10 mutations. May 2006. 16th Meeting of the European Neurological Society, Lausanne, Switzerland. (Oral presentation)
2. K. Inoue, M. Khajavi, C. Akazawa, K. Deguchi, J.R. Lupski. Molecular mechanisms underlying human *SOX10* mutations causing distinct neurocristopathies. August 2006. 16th Biennial Meeting of the International Society for Developmental Neuroscience, Banff, Canada.
3. K. Takano, E. Nakagawa, K. Inoue, F. Kamada, S. Kure, Y. Goto. A loss-of-function mutation in the *FTSJ1* gene causes non-syndromic mental retardation in a Japanese family. October 2006. 56th annual meeting of the American Society

of Human Genetics, New Orleans, LA.

4. Hoshi, M., Akazawa, C. and Kohsaka, S. The reduction of the enteric neural crest cells in the nerve growth factor receptor, p75, knockout mice. 15th International Society of Developmental Biologists Congress. Sydney, Australia, July 7, 2006.
5. 赤澤智宏、佐々木洋、星雅人、中村泰子、高坂新一　顔面神経損傷によって発現誘導される新規の4回膜貫通型蛋白の生化学的解析　第29回日本神経科学大会、2006年7月20日、京都
6. S KOIZUME, S Takizawa, S Yamashita, Y Miyagi, H Osaka. Aberrant trafficking of a mutated proteolipid protein in a mild Pelizaeus-Merzbacher disease. 第20回国際生化学・分子生物学会議/2006年6月18日 京都
7. K. Deguchi, S. Takashima, D. Armstrong, K. Inoue. Impaired neural progenitor cells in extremely preterm infants may affect cortical development and function. May 2006.16th Meeting of the European Neurological Society, Lausanne, Switzerland.
8. K. Deguchi, S. Takashima, D.L. Armstrong, K. Inoue. Neural progenitor cells are impaired in extremely preterm infants with ischemic brain injuries. August 2006. 16th Biennial Meeting of the International Society for Developmental Neuroscience, Banff, Canada.
9. **井上　健**. Nonsense mediated mRNA decay as a modifier of neurological disease traits and phenotypes. 2007年9月11日. Neuro2007. 横浜
10. **K. Inoue**, T. Ohyama, Y. Sakuragi, L-H Yu, R. Yamamoto, Y. Goto, M. Wegner, J.R. Lupski. Translation of *SOX10* 3' untranslated region causes a complex severe neurocristopathy by generation of a deleterious functional domain. Oct 25, 2007. 57th Annual meeting of the American Society of Human Genetics, San Diego, CA.
11. **井上　健**、余　荔華、出口貴美子、岩下晴美、山本良子、Barbara Antalfy、小坂　仁、伊藤雅之、後藤雄一 Pelizaeus-Merzbacher病の病態に基づく治療法開発の試み　第52回日本人類遺伝学会　2007年9月13日　東京

12. 赤澤智宏、中村泰子、前野浩志、和田圭司、高坂新一．恐怖条件付けによって扁桃体で発現上昇するポロキナーゼ Snk の脳内発現．第 30 回日本神経科学大会、第 50 回日本神経化学会大会、第 17 回日本神経回路学界大会合同大会．平成 19 年 9 月 11 日、横浜．
13. 赤澤智宏、橋本学、高坂新一．ソニックヘッジホッグによる神経栄養因子を介した神経再生．精神・神経疾患委託費「中枢神経系の温存的神経再生療法の確立に関する開発的研究」班会議．平成 19 年 12 月 3 日、大阪．
14. H OSAKA et al. Distinct clinical course of SMEI with SCN 2A mutation-Comparison with SCN 1A mutations. 10th Annual Meeting of the Infantile Seizure Society; INTERNATIONAL SYMPOSIUM ON BIOLOGY OF SEIZURE SUSCEPTIBILITY. April 7 2007, Tokyo
15. 小坂仁ら Pelizaeus-Merzbacher 病の病態解析 49 回日本小児神経学会総会 5 月 5-7 日 2007, 大阪
16. Deguchi K. Extremely preterm infants with white matter injury: impaired neural progenitor cells and cortical development. 35th Japanese Fetal and Neonatal Neurological Conference (Osaka, Tokyo)
17. K. Inoue. PCWH-a complex neurocristopathy caused by SOX10 mutation. 2008,9,16. 2nd International SOX meeting 淡路島
18. K. Inoue, T. Ohyama, Y. Sakuragi, R. Yamamoto, NA. Inoue, L-H. Yu, Y. Goto, M. Wegner, J.R. Lupski. Translation of *SOX10* 3' untranslated region causes a complex severe neurocristopathy by generation of a deleterious functional domain. Jun 9, 2008. 18th Meeting of the European Neurological Society, Nice, France
19. Inoue, K. Takano, Y. Goto. Nonsense-mediated mRNA decay may be involved in the down-regulation of the *Alu*-containing splicing variants. Nov 13 2008. 58th Annual meeting of the American Society of Human Genetics, Philadelphia, USA
20. 余荔華、岩下晴美、山本良子、出口貴美子、B. Antalfy、井上直子、伊藤雅之、後藤雄一、小坂仁、井上健 クルクミン：モデルマウスを用いた Pelizaeus-Merzbacher 病の治療法開発の試み 第 5 3 回日本人類遺伝学会 2008 年 9 月 28 日 東京

21. 井上健、桜木陽介、山本良子、井上直子、後藤雄一、JR Lupski SOX10 遺伝子変異による複合型神経堤症候群 PCWH の分子病態の解明　第 5 3 回日本人類遺伝学会 2008 年 9 月 30 日　東京
22. 井上健、赤澤智宏、山本良子、井上直子、Lupski, JR. PCWH-新たな遺伝性ミエリン疾患をとりまく SOX10 変異の分子病態メカニズム. 第 31 回日本神経科学大会. 2008, 7, 9 東京国際フォーラム
23. 石井邦弥、橋本学、中村泰子、高坂新一、赤澤智宏. BDNF を介したソニックヘッジホッグによる損傷神経修復. 第 31 回日本神経科学大会. 2008, 7, 9 東京国際フォーラム
24. 松尾望、石井邦弥、亀谷富由樹、荒木亘、高坂新一、赤澤智宏. Class C-Vps 複合体による細胞内 BACE 蛋白の制御機構. 第 31 回日本神経科学大会. 2008, 7, 9 東京国際フォーラム.
25. 赤澤智宏、井上高良、井上健、井上由紀子、高坂新一. VENUS-SOX10 トランスジェニックマウスを用いた神経堤細胞の分化・増殖・移動のイメージング. 第 31 回日本神経科学大会. 2008, 7, 9 東京国際フォーラム.
26. 小坂仁、黒澤健司、井合瑞江、山田美智子、山下純正 Pelizaeus-Merzbacher 病の治療薬スクリーニング系の作成 第 50 回日本小児神経学会総会　平成 20 年 5 月 30 日東京
27. 小坂仁 、辻 恵、高木篤史、鮫島希代子、井合瑞江、山下純正 多発性硬化症類似の中枢神経病変を示す Charcot-Marie-Tooth 病の 1 例 第 49 回関東小児神経学会　平成 20 年 9 月 20 日静岡
28. 小坂仁、黒澤健司、井合瑞江、山田美智子、山下純正 Pelizaeus-Merzbacher 病の治療 第 50 回日本先天代謝異常学会総会　平成 20 年 10 月 30 日米子
29. Deguchi K., Antalffy B., Takei H., Powell S., Yamamoto R., D' Arcangelo G., Inoue K. A neuronal migration regulator Reelin pathway may be involved in the white matter pathology in Alzheimer's disease. Jun 10, 2008. 18th Meeting of the European Neurological Society, Nice, France

G. 健康危険情報

特記事項無し

H. 知的財産権の出願・登録状況

「神経堤細胞のライブイメージングマウス」発明者：赤澤智宏、共同発明者：高坂新一、井上健、井上高良
出願中

研究成果の刊行に関する一覧表

書籍

著者氏名	論文タイトル名	書籍全体の編集者名	書籍名	出版社名	出版地	出版年	ページ
Inoue K	Pelizaeus-Merzbacher disease and spastic paraplegia type 2: mechanistic similarities with and differences from Charcot-Marie-Tooth disease type 1A/heredirary neuropathy with liability to pressure palsies.	Stankiewicz P, Lupski JR,	Genomic Disorder: The Genomic Basis of Disease	Humana Press	Totowa	2006	263-272
井上　健	ゲノミクス・機能的ゲノミクス・エピジェネティクス—精神遅滞との関連	モイラスミス（著）後藤雄一（監訳）	精神遅滞と発達の遅れ	診断と治療社	東京	2007	142-159
Shiga K, **Inoue K,** Lupski JR.	Mendelian, Non-mendelian, multigenetic inheritance and complex traits	Rosenberg RN, Prusiner SB, DiMauro S, Barchi RL, Nestler EJ	The Molecular and Genetic Basis of Neurological and Psychiatric Disease 4th edition	Butter Heinemann	Philadelphia PA	2007	
井上　健	遺伝子治療の最前線	有馬正高、加我牧子、稲垣真澄	小児神経学	診断と治療社	東京	2008	510-511

Osaka, H., Mazaki, E., Okamura, N., Iai, M., Yamada, M., Yamakawa, K., Yamashita, S.	Distinct clinical course of epilepsy with an SCN2A mutation-comparison with SCN1A mutations.	Takao Takahashi, Yukio Fukuyama	Biology of Seizure Susceptibility in Developing Brain. Progress in Epileptic Disorders Series, Vol. 6	John Libbey Eurotext	Montrouge (Paris) France	2008	87-100
小坂　仁	Pelizaeus-Merzbacher 病	小児内科編集部	小児中枢神経疾患の画像診断	東京医学社	東京	2008	484-85
小坂仁、黒澤健司、井合瑞江、山下純正	Pelizaeus-Merzbacher 病の遺伝子診断	辻省次	神経内科	科学評論社	東京	2008	印刷中
森麻子、赤澤智宏	腎疾患・透析・尿路疾患	松浦雅人	臨床病態学	医歯薬出版	東京	2009	未定

雑誌

発表者氏名	論文タイトル名	発表誌名	巻号	ページ	出版年
Lee JA, Madrid RE, Sperle K, Ritterson CM, Hobson GM, Garbern J, Lupski JR, Inoue K.	Spastic paraplegia type 2 associated with axonal neuropathy and apparent *PLP1* position effect.	*Ann Neurol*	59(2)	398-403.	2006
Lee JA, Inoue K, Cheung SW, Shaw CA, Stankiewicz P, Lupski JR.	Role of genomic architecture in *PLP1* duplication causing Pelizaeus-Merzbacher disease.	*Hum Mol Genet*	15(14)	2250-2265	2006
Kim, B. Y., Sahara, Y., Yamamoto, A., Kominami, E., Kohsaka,	The interaction of mammalian Class C Vps with nSec-1/Munc18-a	*Biochem. Biophys. Res. Comm.*	350	691-697	2006

S., and Akazawa, C.	and syntaxin 1A regulates presynaptic release.				
Yogosawa, S., Kawasaki, M., Wakatsuki, S., Kominami, E., Shiba, Y., Nakayama, K., Kohsaka, S. and Akazawa, C.	Monoubiquitylation of GGA3 by hVPS18 regulates its ubiquitin-binding ability.	*Biochem. Biophys. Res. Comm.*	350	82-90	2006
Koizume, S., Takizawa, S., Fujita, K., Aida, N., Yamashita, S., Miyagi, Y., and Osaka, H	Aberrant trafficking of a proteolipid protein in a mild Pelizaeus-Merzbacher disease.	*Neuroscience*	141	1861-1869 .	2006
Sato, A., Arimura, Y., Manago, Y., Nishikawa, K., Aoki, K., Wada, E., Suzuki, Y., Osaka, H., Setsuie, R., Sakurai, M., *et al.*	arkin potentiates ATP-induced currents due to activation of P2X receptors in PC12 cells.	*J Cell Physiol.*	209	172-182	2006
Sun, Y. J., Nishikawa, K., Yuda, H., Wang, Y. L., Osaka, H., Fukazawa, N., Naito, A., Kudo, Y., Wada, K., and Aoki, S. (2006).	Solo/Trio8, a membrane-associated short isoform of Trio, modulates endosome dynamics and neurite elongation.	*Mol Cell Biol*	26	6923-6935	2006
Wang, Y. L., Liu, W., Sun, Y. J., Kwon, J., Setsuie, R., Osaka, H., Noda, M., Aoki, S., Yoshikawa, Y., and Wada, K.	Overexpression of ubiquitin carboxyl-terminal hydrolase L1 arrests spermatogenesis in transgenic mice.	*Mol Reprod Dev*	73	40-49	2006
Takahashi, Y, Matsuda, K, Kubota Y, Shimomura J, Yamasaki, E, Kudo, T, Fukushima K, Osaka H, Akasaka N, Imamaura , A, Yamada, S, Kondo, N, Fujiwara, T	Vaccination and infection as causative factors in Japanese patients with Rasmussen syndrome: Molecular mimicry and HLA class I	*Clin Dev Immunol.*	13	381–387	2006
Setsuie, R., Wang, Y. L., Mochizuki, H., Osaka, H., Hayakawa, H., Ichihara, N., Li, H., Furuta, A., Sano, Y., Sun, Y. J., *et al.*	Dopaminergic neuronal loss in transgenic mice expressing the Parkinson's disease-associated UCH-L1 I93M mutant.	*Neurochem Int.*	50(1)	119-129	2007

Inoue K, Ohyama T, Sakuragi Y, Yamamoto R, Inoue NA, Yu L-H, Goto YI, Wegner M, Lupski JR.	Translation of SOX10 3' untranslated region causes a complex severe neurocristopathy by generation of a deleterious functional domain.	*Hum Mol Genet.*	16	3037-46	2007
Ohsawa, K., Irino, Y., Nakamura, Y., Akazawa, C., Kohsaka, S.	Involvement of P2X4 and P2Y12 receptors in ATP-induced microglial chemotaxis.	GLIA	55	604-616	2007
Kim, B. Y. Akazawa, C.	Endosomal trafficking of EGFR regulated by hVps18 via interaction of MVB sorting machinery	Biochem. Biophys. Res. Comm.			in press
赤澤智宏、高坂新一.	末梢神経の再生におけるソニックヘッジホッグの役割	BRAIN and NERVE	59	1341-1346	2007
Setsuie, R., Wang, Y. L., Mochizuki, H., Osaka, H., Hayakawa, H., Ichihara, N., Li, H., Furuta, A., Sano, Y., Sun, Y. J., *et al.*	Dopaminergic neuronal loss in transgenic mice expressing the Parkinson's disease-associated UCH-L1 I93M mutant.	*Neurochem Int.*	50(1)	119-129	2007
Osaka H, Ogiwara I, Mazaki E, Okamura N,Yamashita S, Iai M, et al.	Patients with a sodium channel alpha 1 gene mutation show wide phenotypic variation.	*Epilepsy Res*	75	46-51	2007
Tohyama J, Akasaka N, Osaka H, Maegaki Y, Kato M, Saito N, et al.	Early onset West syndrome with cerebral hypomyelination and reduced cerebral white matter.	*Brain Dev*			*in press*
Hirano R, Interthal H, Huang C, Nakamura T, **Deguchi K**, Choi K, Bhattacharjee MB, Arimura K, Umehara F, Izumo S, Northrop JL, Salih MAM, **Inoue K,**	Spinocerebellar ataxia with axonal neuropathy: consequence of a Tdp1 recessive neomorphic mutation?	*EMBO J*	26	4732-43	2007

Armstrong DL, Champoux JJ, Takashima H, Boerkoel CF					
Deguchi K, Clewing JM, Elizondo LI, Hirano R, Huang C, Choi K, Sloan EA, Lücke T, Marwedel KM, Powell RD, SantaCruz K, Willaime-Morawek S, **Inoue K**, Lou S, Northrop JL, Kanemura Y, van der Kooy D, Okano H, Armstrong DL, Boerkoel CF.	Neurological phenotype of Schimke immuno-osseous dysplasia and neurodevelopmental expression of SMARCAL1.	*J Neuropath Exp Neurol*	67	565-77	2008
Takano K, Nakagawa E, **Inoue K**, Kamada F, Kure S, Goto YI; Japanese Mental Retardation Consortium	A loss-of-function mutation in the *FTSJ1* gene causes nonsyndromic X-linked mental retardation in a Japanese family.	Am J Med Genet B Neuropsychiatr Genet.	147B(4)	479-84	2008
Elizondo LI, Cho KS, Zhang W, Yan J, Huang C, Huang Y, Choi K, Sloan EA, **Deguchi K**, Lou S, Baradaran-Heravi A, Takashima H, Lücke T, Quiocho FA, Boerkoel CF.	Schimke immuno-osseous dysplasia: SMARCAL1 loss-of-function and phenotypic correlation.	J Med Genet.	46(1)	49-59	2009
Goto, A., Wang, Y. L., Kabuta, T., Setsuie, R., **Osaka, H.**, Sawa, A., Ishiura, S., and Wada, K.	Proteomic and histochemical analysis of proteins involved in the dying-back-type of axonal degeneration in the gracile axonal dystrophy (gad) mouse.	Neurochem Int.	*in print*		2008
Saitsu, H., Kato, M., Mizuguchi, T., Hamada, K., **Osaka, H.**, Tohyama, J., Uruno, K., Kumada, S., Nishiyama, K., Nishimura, A., *et al.*	De novo mutations in the gene encoding STXBP1 (MUNC18-1) cause early infantile epileptic encephalopathy.	Nat Genet	40	782-788.	2008
Tanaka, M., Hamano, S., Sakata, H., Adachi, N.,	Discrepancy between auditory brainstem	Auris Nasus	35	404-407.	2008

Kaga, K., **Osaka, H.**, and Kurosawa, K.	responses, auditory steady-state responses, and auditory behavior in two patients with Pelizaeus-Merzbacher disease.	Larynx			
Liang C, Lee JS, Inn KS, Gack MU, Li Q, Roberts EA, Vergne I, Deretic V, Feng P, **Akazawa C**, Jung JU	Beclin 1-binding UVRAG targets the class C Vps complex to coordinate autophagosome maturation and endocytic trafficking.	Nature Cell Biology	10(7)	776-787	2008
Hashimoto M, Ishii K, Nakamura Y, Watabe K, Kohsaka S, **Akazawa C**	Neuroprotective effect of Sonic hedgehog up-regulated in Schwann cells following sciatic nerve injury.	J Neurochemistry	107(4)	918-927	2008
志村健作、石井邦弥、松尾望、赤澤智宏	BAC トランスジェニックマウス作成法を用いた Neural Crestopathy（神経堤関連疾患）解析の新規モデルマウス作成	順天堂医学	In press		

研究成果の刊行物・別刷（抜粋）

Human Molecular Genetics, 2006, Vol. 15, No. 14 **2250–2265**
doi:10.1093/hmg/ddl150
Advance Access published on June 14, 2006

Role of genomic architecture in *PLP1* duplication causing Pelizaeus-Merzbacher disease

Jennifer A. Lee[1], Ken Inoue[3], Sau W. Cheung[1], Chad A. Shaw[1], Pawel Stankiewicz[1] and James R. Lupski[1,2,4,*]

[1]Department of Molecular and Human Genetics, [2]Department of Pediatrics, Baylor College of Medicine, One Baylor Plaza, Room 604B, Houston, TX 77030, USA, [3]Department of Mental Retardation and Birth Defect Research, National Institute of Neuroscience, National Center of Neurology and Psychiatry, Kodaira, Tokyo 187-8502, Japan and [4]Texas Children's Hospital, Houston, TX 77030, USA

Received April 18, 2006; Revised and Accepted June 6, 2006

Genomic architecture, higher order structural features of the human genome, can provide molecular substrates for recurrent sub-microscopic chromosomal rearrangements, or may result in genomic instability by forming structures susceptible to DNA double-strand breaks. Pelizaeus-Merzbacher disease (PMD) is a genomic disorder most commonly arising from genomic duplications of the dosage-sensitive proteolipid protein gene (*PLP1*). Unlike many other genomic disorders that result from non-allelic homologous recombination utilizing flanking low-copy repeats (LCRs) as substrates, generating a common and recurrent rearrangement, the breakpoints of *PLP1* duplications have been reported not to cluster, yielding duplicated genomic segments of varying lengths. This suggests a distinct molecular mechanism underlying *PLP1* duplication events. To determine whether structural features of the genome also facilitate *PLP1* duplication events, we analyzed extensively the genomic architecture of the *PLP1* region and defined several novel LCRs (LCR–PMDs). Array comparative genomic hybridization showed that *PLP1* duplication sizes differed, but revealed a subgroup of patients with apparently similar *PLP1* duplication breakpoints. Pulsed-field gel electrophoresis analysis using probes adjacent to the LCR–PMDs detected unique recombination-specific junction fragments in 12 patients, enabled us to associate the LCR–PMDs with breakpoint regions, and revealed rearrangements inconsistent with simple tandem duplications in four patients. Two-color fluorescence *in situ* hybridization was consistent with directly oriented duplications. Our study provides evidence that *PLP1* duplication events may be stimulated by LCRs, possibly non-homologous pairs at both the proximal and distal breakpoints in some cases, and further supports an alternative role of genomic architecture in rearrangements responsible for genomic disorders.

INTRODUCTION

Architectural features of the human genome can result in genome instability, and susceptibility to rearrangements resulting in disease traits. Such rearrangements, including deletions, duplications and inversions at specific regions may result in the loss or gain of a dosage-sensitive gene (or genes), disruption of a gene, generation of a novel gene at the breakpoints, or dysregulation of a gene in proximity to the rearrangement, causing what is termed a genomic disorder (1–3). Genomic disorders represent a wide spectrum of unrelated clinical conditions including, for example, Charcot-Marie-Tooth disease type 1A (4,5), Smith-Magenis syndrome (6,7) and Williams syndrome (8,9). Yet, the underlying molecular basis is the same: rearrangement involving specific genomic segments ranging from a few kilobases (kb) to several megabases (Mb) in length (10). Many genomic disorders share a common mechanism for their underlying rearrangement: non-allelic homologous recombination (NAHR) between low-copy repeats (LCRs) that flank the rearranged genomic segment (1). Such rearrangements yield common recombinant genomic segments. However, some

*To whom correspondence should be addressed. Tel: +1 7137983723; Fax: +1 7137985073; Email: jlupski@bcm.tmc.edu

genomic disorders, and selected rearrangements for specific genomic disorders, that deviate from this classic model exist.

Among them is Pelizaeus-Merzbacher disease (PMD), a rare X-linked dysmyelinating disorder of the central nervous system (CNS) (11–13). PMD most commonly (60–70%) arises from genomic duplications of the dosage-sensitive proteolipid protein gene (*PLP1*) (14,15) located on chromosome Xq22.2 (16,17), and less commonly by *PLP1* deletions (18) and point mutations (11). Both the deletions (18) and duplications (19) causing PMD appear to arise by non-homologous end joining (NHEJ) as surmised from the nucleotide sequence of the products of recombination. However, what makes the genomic region surrounding *PLP1* susceptible to rearrangement remains to be elucidated. PLP1 is an integral membrane protein and the most abundant component of myelin in the CNS; an extra copy of *PLP1* resulting from whole gene duplication affects the development of oligodendrocytes. Specifically, PMD caused by *PLP1* duplication is characterized by oligodendrocyte cell death and abnormal CNS myelination (20).

Many genomic disorders result from homologous recombination between non-allelic LCRs, yielding recombination products with common breakpoints. Interestingly, in PMD patients with *PLP1* duplication, the rearrangement breakpoints are not common, yielding duplicated genomic segments of varying lengths (14,21). This suggests that the molecular mechanism underlying *PLP1* duplication events is likely distinct from the more common NAHR mechanism. We hypothesized that various LCRs in the PMD region might stimulate DNA rearrangements resulting in *PLP1* gene duplication, because complex genomic architecture can cause genomic instability and predispose chromosomal rearrangements (1,2,22) and as LCRs are thought to catalyze non-recurrent rearrangements (23). We therefore performed an extensive bioinformatic analysis of this region and mapped the breakpoints in multiple PMD patients with duplication of *PLP1*. Interestingly, we found that although the duplications differ in size, they appear to cluster into groups of similar size. The rearrangement breakpoints in these groupings appear to be in proximity to unusual genome architecture.

RESULTS

Numerous LCRs identified in the region surrounding *PLP1*

Extensive *in silico* analysis of an ~8 Mb region (Build 35: 98 358 000–106 357 999; Xq22.1-q22.3) uncovered several novel LCRs proximal to *PLP1*, whereas the distal LCRs included only LCR–PMDA through D (Fig. 1). We previously defined the structures LCR–PMDA and B as two inverted repeats, each with two homologous segments: A1a and A2 for LCR–PMDA, and A1b and A3 for LCR–PMDB (18); LCR–PMDC and D were more recently defined by Woodward *et al.* (19) as distal LCRs which flank LCR–PMDA and B. The novel LCRs have greater than 89% identity and are at least 500 bp in length. Compared with similar analyses of the Charcot-Marie-Tooth disease type 1A (4,24), Smith-Magenis syndrome (23,25,26) and Sotos syndrome (27,28) regions, analyses of the *PLP1* region revealed more complex genome architecture, with a greater diversity in the number, copies and orientations of the constituent LCRs surrounding the dosage-sensitive gene *PLP1*.

LCRs with shared homology were discovered only within the 3 Mb region surrounding *PLP1* (Fig. 1). Inter-chromosomal LCRs with homology to regions on various autosomes and chromosome Y, and intra-chromosomal LCRs with homology to other non-adjacent regions on chromosome X were excluded from further analysis. Novel LCRs located ~1.4 Mb proximal to *PLP1*, which we termed LCR–PMDF1 and F2 (Figs 1 and 2, Table 1), represent a set of large LCRs in inverted orientation, each spanning ~122 kb with 99.9% shared sequence identity. LCRs identified nearest to *PLP1* are situated ~276 kb proximal (LCR–PMDE2) and ~125 kb distal (LCR–PMDC) to the gene (Fig. 1, Table 1). Other LCRs in this 3 Mb region (Fig. 1), with their sizes, positions and percent identities, are as shown in Figure 2 and Table 1. There are LCRs in the vicinity of proximal and distal breakpoints of *PLP1* duplications in PMD patients delineated by fluorescence *in situ* hybridization (FISH) mapping (14), including 11 patients reported herein; therefore, we focused on these particular genomic regions for more in-depth analyses of their potential role in *PLP1* duplication events.

Duplication breakpoints are diverse but appear to cluster into groups

In all patients (Table 2) whose *PLP1* duplication has been confirmed by FISH, custom array comparative genomic hybridization (CGH) analysis revealed their duplication sizes at a bacterial artificial chromosome (BAC) and P1 artificial chromosome (PAC) clone resolution (Fig. 3). We detected duplications which covered the span of one or two BAC clones (~180–250 kb), as well as larger duplications (~4–7 Mb), some of which extend distal to *PLP1* beyond the detection range of the array (over 7 Mb). Of the five patients with larger duplications (Table 2), two have cytologically visible duplications by G-banding: BAB2396 [46,XY,dup(X)(q22.1q22.2)] and BAB2425 [46,XX,dup(X)(q22.1q22.3)] (Supplementary Material, Fig. S1). Siblings BAB2389 and 2390 (from family HOU893), have a duplication estimated to be ~4 Mb in size, and their duplication was not cytologically visible; BAB1327 was not analyzed by G-banding.

Interestingly, there appears to be a subgroup of 15 patients (12 families) who have similar proximal and/or distal breakpoints at a BAC/PAC resolution (Figs 3 and 4). This subgroup represents ~71% of our patient cohort (15/21), or 71% of families (12/17), and ~72% of breakpoints (23/32) for the families we report herein. For this subgroup, custom array CGH often revealed four to five BAC clones duplicated (~650 kb), generally including BACs RP11-1123D8, RP11-1144F22, RP11-832L2 (*PLP1*), RP11-34P3 and RP11-462K21 (Fig. 3). Some end clones appear to be partially duplicated because of their intermediate signal intensity, indicating that the breakpoint likely occurs within that particular clone (duplication end clone), whereas others are completely duplicated, suggesting that the breakpoint either occurs within that clone, and/or within the adjacent overlapping clone (duplication end-clone pair).

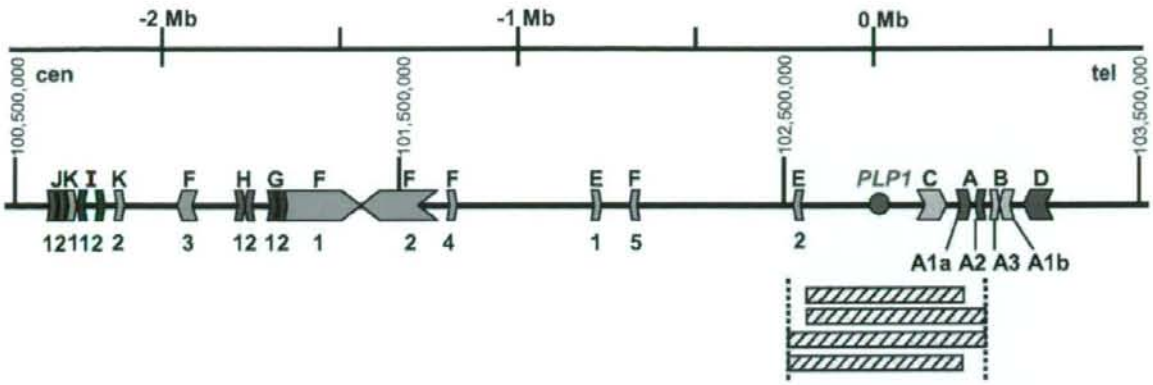

Figure 1. *In silico* analysis reveals LCRs in the 3 Mb region surrounding *PLP1*. Novel LCRs, having pair-wise alignments with greater than 89% identity, are displayed centromeric (cen) to telomeric (tel). Those with shared identity are shown graphically in like colors; the direction of the block arrows indicates the relative orientation. The large orange block arrows, LCR–PMDF1 and F2, contain numerous short subunits and have shared identity in an inverted orientation. The smaller orange LCRs are labeled LCR–PMDF3, F4 and F5; all LCR–PMDFs have shared identity. LCR–PMDG1 and G2 (maroon), LCR–PMDJ1 and J2 (magenta) and LCR–PMDK1 and K2 (pink) are directly oriented LCRs that have shared identity, respectively; LCR–PMDH1 and H2 (brown), LCR–PMDE1 and E2 (light green) and LCR–PMDI1 and I2 (dark purple) are inverted LCRs that have shared identity, respectively. LCR–PMDA (dark blue), LCR–PMDB (light blue), LCR–PMDC (yellow) and LCR–PMDD (dark green) are shown. The *PLP1* gene is indicated by the red circle, and genomic positions are given relative to the *PLP1* gene in megabases. Alignment with representative *PLP1* duplications falling within a subgroup having similar proximal and distal breakpoints is shown (striped bars within vertical dotted lines). The exact size and shared percent identity for these LCRs are given in Table 1 and Figure 2, respectively.

	A1a	A2	A3	A1b	C	D	E1	E2	F1	F2	F3	F4	F5	G1	G2	H1	H2	I1	I2	J1	J2	K1	K2
A1a	100																						
A2	87.8	100																					
A3	89.8	86.8	100																				
A1b	98.9	87.8	89.9	100																			
C					100																		
D					92.7	100																	
E1							100																
E2							95.0	100															
F1									100														
F2									99.9	100													
F3									95.4	95.3	100												
F4									94.2	94.2	94.2	100											
F5									93.4	93.4	93.4	92.9	100										
G1									93.1	93.1				100									
G2									100	99.9				93.1	100								
H1																100							
H2																92.2	100						
I1																		100					
I2																		99.9	100				
J1																				100			
J2																				89.7	100		
K1																						100	
K2																						89.5	100

Figure 2. Grid of cumulative percent identities of all alignments for each LCR–PMD pair. White squares contain percent identity shared among LCRs from horizontal and vertical axes. Grey squares indicate pairs of LCRs which have no significant indentity.

Breakpoint groupings are coincident with complex architecture

After determining which of the custom array CGH clones contain LCRs (Table 1), we sought to determine if the breakpoints of the above subgroup of PMD patients who appear to have similar proximal and/or distal breakpoints at a BAC/PAC resolution (Figs 3 and 4) occur within or near LCR-containing clones to test the hypothesis that LCR–PMDs are stimulating, but not necessarily mediating, these rearrangements. From this analysis, we identified the following LCR-containing clones at or near the breakpoints: RP11-1123D8 (LCR–PMDE2),

Table 1. LCR–PMDs from previous and present *in silico* analyses

LCR–PMD	BAC(s) within	Size (kb)	Position (Build 35)	Orientation
AA1a	*RP11-462K21*	18.5	103,029,820-103,048,307	(+)
AA2	*RP11-462K21*	10.3	103,064,260-103,074,533	(−)
BA3	*RP11-462K21*	13.9	103,096,154-103,110,142	(+)
BA1b	*RP11-462K21*	18.5	103,111,984-103,130,746	(−)
C	*RP11-34P3*	34.8	102,978,791-103,013,644	(+)
D	*RP11-462K21*	26.9	103,137,452-103,164,433	(−)
E1	RP11-155E24	2.4	101,998,037-102,000,480	(+)
E2	*RP11-1123D8*	2.4	102,559,737-102,562,186	(−)
F1	RP11-461E24	121.9	101,276-701-101,398,620	(+)
F2	RP11-669M24	121.9	101,410,623-101,532,603	(−)
F3	CTD-2006G2	8.4	100,898,811-100,907,221	(−)
F4	CTD-2131P19	1.4	101,625,289-101,626,682	(+)
F5	RP11-1061F13	1.3	102,141,897-102,143,193	(−)
G1	RP11-165B8, RP11-461C20	11.3	101,234,198-101,245,515	(+)
G2	RP11-461C20	4.8	101,282,660-101,287,458	(+)
H1	RP11-165B8	0.9	101,187,082-101,187,979	(+)
H2	RP11-165B8	0.9	101,202,419-101,203,313	(−)
I1	RP11-66I17	4.5	100,658,634-100,663,108	(−)
I2	RP11-66I17	4.5	100,672,941-100,677,415	(+)
J1	RP11-15E22	0.7	100,557,050-100,557,755	(+)
J2	RP11-15E22	0.7	100,615,928-100,616,623	(+)
K1	RP11-15E22	0.6	100,621,785-100,622,389	(+)
K2	RP11-15E22	0.7	100,689,999-100,690,668	(+)

LCR-containing BAC clones listed are from those on our CGH array. Sets of LCRs are designated by LCR-PMD letter, with the following previously published exceptions: *A* and *B* are a set of four LCRs (18), and *C* and *D* are a set of two LCRs (19). Relative orientation within each set of related LCRs assigned as (+) or (−). LCRs and BACs in italics are those which are present at/near the breakpoints in a subset of patients with similar breakpoints at a BAC/PAC resolution.

Table 2. Cohort of patients included in the present study

Family (HOU#)	Patient (BAB#)	Sex
485	1258[d]	M
487	1263[a,d]	M
	1264[a,d]	M
587	1482[b]	M
	1597[b]	M
519	1334[d]	M
674	1705[a]	M
	1707[a]	M
503	1305[d]	M
501	1301[d]	M
944	2448[c]	M
486	1261[d]	M
494	1282[d]	M
491	1275[d]	M
497	1290[d]	M
561	1420	M
893	2389[a,c]	M
	2390[a,c]	M
924	2396[c]	M
516	1327[c,d]	M
936	2425[c]	F

[a]Siblings within the same family, as listed by HOU#.
[b]Cousins within the same family.
[c]Larger duplication patients (at least ~4 Mb).
[d]Clinical details previously published (14).
[e]Clinical details previously published (47).

RP11-34P3 (LCR–PMDC) and RP11-462K21 (LCR–PMDA, B, and D), which range from 132 to 192 kb in length (average being 146.5 kb). The latter clone is also found at the distal breakpoint for some larger-sized *PLP1* duplications. In a BLAST 2 analysis of the individual breakpoint-spanning clones (Fig. 3), we did not find any additional stretches of >200 bp that shared >85% identity.

We calculated the number of breakpoints that occur within an LCR-containing BAC or PAC duplication end clone or duplication end-clone pairs, versus the number of breakpoints that occur within non-LCR clones. Considering only families with at least one similar breakpoint, we determined that 92% of proximal breakpoints (11/12) and 92% of distal breakpoints (11/12) occur within LCR-containing duplication end clones or duplication end-clone pairs. Considering both proximal and distal breakpoints together, 92% of the breakpoints (22/24) occur within LCR-containing duplication end clones or duplication end-clone pairs for this subgroup. Analyzing the aggregate data from all families in our cohort, 71% of proximal breakpoints (12/17) and 87% of distal breakpoints (13/15) occur in an LCR-containing end clone or end-clone pair. We included only 15 total distal breakpoints (and 32 total breakpoints) because the duplications in two patients (BAB2396 and 2425; Fig. 3) extend distally beyond the genomic region detected by our custom array.

On our array, 14 of the 68 tiled BAC and PAC clones contain LCR–PMDs (Table 1). When we compared the frequency of families with at least one breakpoint in an LCR-containing end clone or end-clone pair ($12/17 = 0.7059$) with the frequency of LCR-containing clones on the full-length array ($14/68 = 0.2059$), the observed frequency is significantly higher, with a P-value of 1.255×10^{-5}. The P-value was determined by performing a binomial test of the proportion

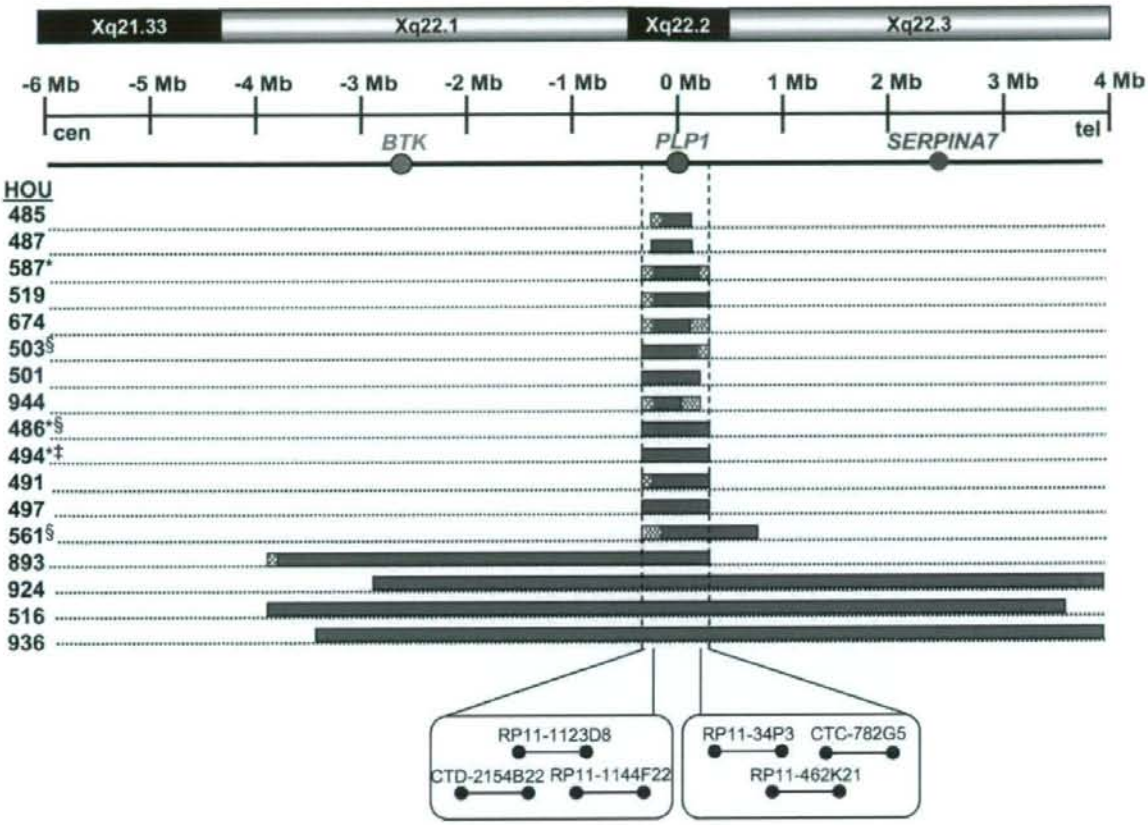

Figure 3. Genomic regions duplicated in our cohort of PMD families analyzed by array CGH. Note the grouping of breakpoints in a subset of patients, delineated by vertical dotted lines; graphical normalized data for these patients are displayed in this figure. Duplication regions similar at a BAC/PAC resolution generally include BAC clones RP11-1123D8, RP11-1144F22, RP11-832L2, RP11-34P3 and RP11-462K21; RP11-832L2 contains the full-length *PLP1* gene. Patients in families HOU924 and 936 have large duplications that extend beyond the region detected by the ~10 Mb array. Representative data for each family are listed by HOU#; those denoted by an asterisk are further discussed in Figure 6; those denoted by a section symbol are complex rearrangements; and that denoted by a dagger symbol is an interrupted direct duplication. Solid blue bars represent clones for which the mean normalized $\log_2$(Cy3/Cy5) ratio of the CGH signal reached a threshold of at least 0.2, except for families HOU501, 516 and 936 for which the ratio approached the threshold yet still represent copy number gains; their duplication sizes were confirmed independently by FISH. Checkered blue bars represent partially duplicated end clones. The boxes below highlight duplication end clones (including single end clones and end-clone pairs) found at the duplication breakpoints. Positions are given relative to the *PLP1* gene (red circle) in megabases, centromeric (cen) to telomeric (tel), and the chromosomal band position is shown on top in alternating black and gray bars. *BTK* and *SERPINA7* genes are shown as green and blue circles, respectively, as a reference.

of observed breakpoints in LCR-containing end clones or end-clone pairs, and the *P*-value is exact.

Probes adjacent to LCRs detect junction fragments

To further investigate whether these LCRs may stimulate the genomic rearrangements resulting in *PLP1* duplication, we examined for an association between breakpoint genomic position and co-localization of an LCR. For this, we employed pulsed-field gel electrophoresis (PFGE) analysis followed by hybridization with a series of DNA probes complementary to unique sequences adjacent to LCRs neighboring *PLP1* (Fig. 5). We examined 15 families in this analysis with two different endonuclease digestions and up to 10 different hybridization probes, which resulted in multiple independent hybridizations per family and a scan that covers a total of ~2 Mb spanning the *PLP1* genomic region. We detected recombination-specific junction fragments in 12 patients in 10 families (Table 3). Similar sized junction fragments, within ~100 kb in size, were observed in eight of 10 families. For example, for hybridization with Distal A probe after *Pme*I digestion, 375 kb junction fragments were observed for families HOU587 and 519; 295 kb junction fragments were observed for families HOU674, 503, 497 and 561; 275 kb junction fragments were observed for families HOU486 and 494 (Table 3). In four patients from three families for which complete restriction mapping by PFGE was possible (Fig. 6), we mapped both the proximal and distal ends of

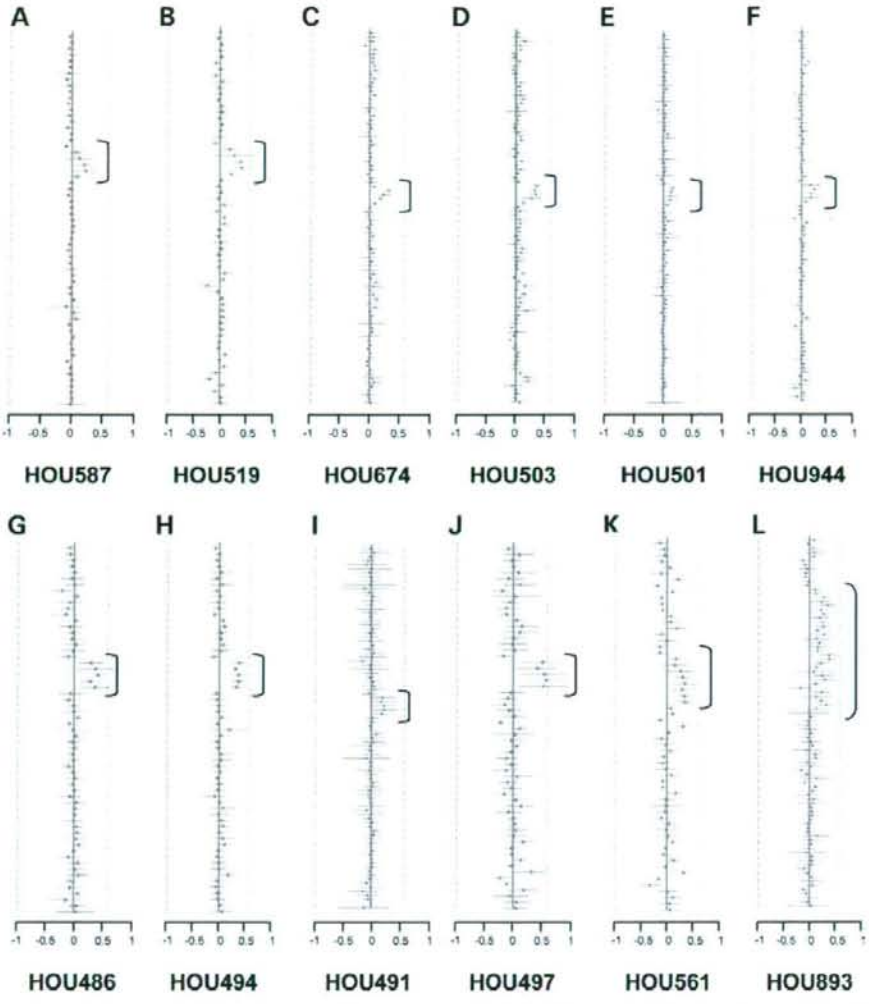

Figure 4. Similar clones duplicated in several PMD patients. Normalized array CGH data for families HOU587, 519, 674, 503, 501, 944, 486, 494, 491, 497, 561 and 893, who have at least one similar breakpoint at a BAC/PAC resolution, are displayed in (**A**–**L**), respectively. For families with more than one affected individual, representative data for only one individual is displayed. As expected, patients in these families appear to have similar proximal and/or distal breakpoints at a BAC/PAC clone resolution. Duplicated regions are indicated by the brackets to the right of each vertical axis. Data from our 38 clone array are displayed in (A, B, G, H, J and K); data from our 68 clone array are displayed in (C–F, I and L).

the *PLP1* duplications. Of all the hybridization probes tested, only Proximal A, B, C, G and Distal A probes identified junction fragments. Distal Probe A is located just proximal to LCR–PMDA (Fig. 5).

For family HOU587, as anticipated, we observed segregation of the junction fragment for all affected and carrier family members, whereas the unaffected male BAB1754 showed only the expected normal band (Fig. 6). Hybridization with Proximal G probe and Distal A probe yielded junction fragments after both *Pme*I and *Nru*I enzyme digestions, whereas hybridization with Proximal C probe yielded junction fragments after *Nru*I digestion. In all junction-positive members of family HOU587, the junction fragments were larger than the expected band sizes, indicating that for the junction fragment, the restriction enzyme sites flanking the hybridization probe are further apart than on non-rearranged DNA (Fig. 5). By restriction enzyme mapping and comparative analysis with reference genome sequence, the duplication is in tandem and is direct in orientation.

In families HOU486 and HOU494, hybridization with Proximal C and Distal A probes yielded junction fragments after *Pme*I digestion, and with Proximal C and G and Distal A probes after *Nru*I digestion. We observed junction fragments of larger than normal-sized bands expected based on restriction maps (Fig. 5) after *Pme*I digestion as described earlier for family HOU587, but of smaller size than the